

Advances in Medical Imaging Applied to Bone Metastases

Àngel González-Sistal¹, Alicia Baltasar Sánchez¹,
Michel Herranz Carnero² and Álvaro Ruibal Morell²

¹*Medical Imaging Research Laboratory, Dpt. Physiological Sciences II
Faculty of Medicine, University of Barcelona*

²*Nuclear Medicine Service, Complejo Hosp. Universitario Santiago de Compostela
Molecular Imaging Group, IDIS
Spain*

1. Introduction

Bone metastases are the result of a primary cancer invasion which spreads into the bone marrow through the lymphogenous or hematogenous pathways. Bone metastases are a common complication of cancer. The primary cancers that most frequently metastasize to bone are breast and prostate cancer (65 - 75 %) amongst many others (thyroid 42 %, lung 36 % or kidney 35 %) (Suva et al., 2011). Although the exact incidence of bone metastases is unknown given its dependence on the type of primary cancer, it is estimated that 350,000 people die of bone metastases annually in the United States.

1.1 Bone structure and microenvironment

Bone is the third most common site of hematogenous tumor metastases after liver and lungs. The imbalance in bone turnover results in a favorable environment for the growth of metastatic tumors, a process known as the vicious cycle of bone metastases (Fili et al., 2009).

Bone consists of cortical, trabecular and marrow components. Cortical bone, is compact and has canals containing vessels. A layer of compact bone surrounds trabecular bone, which contains the bone marrow. Most of the red marrow (hematopoietic) is located in axial bones (spine, ribs, pelvis, proximal femora), whereas fat marrow is found in appendicular bones (long bones). Bone tissue contain the cells types: osteoblasts, osteoclasts, osteocytes and bone-lining cells.

Breast and prostate carcinomas have a great avidity for bone because the molecular interactions between these cancer cells and host cells favor the establishment of osseous lesions. Thyroid, lung, kidney, gastric, colon and skin cancers also metastasize usually to bone but, to a lesser degree, because these cell types do not possess the properties needed for invasion and residence in the bone microenvironment (Weilbaecher et al., 2011).

A number of factors contribute to the high incidence of bone metastases (Eriksen, 2010): high blood flow in the red marrow; adhesive molecules on tumor cells that bind them to marrow stromal cells and bone matrix (tumor cells increase the production of angiogenic

and bone-resorbing factors that further enhance tumor growth in bone); growth factors (transforming growth factor *b* (TGF *b*), insulin-like growth factors I and II (IL-I and IL-II), fibroblast growth factors (FBG), platelet-derived growth factors and bone morphogenetic proteins (BMPs)) that are released and activated during bone resorption, providing fertile ground in which tumor cells can grow (Suva et al., 2009).

The adult skeleton continually turns over and remodels itself. There is a balanced remodeling sequence: osteoclasts resorb bone on trabecular surfaces and then osteoblasts form bone at the same site (Hadjidakis et al., 2006).

1.2 Types and localization of bone metastases

Most tumor implants occur through the hematogenous pathway. The preference for axial involvement is also due to the greater vascularity of the red marrow found in the axial skeleton as opposed to the yellow marrow (high-fat) found in the appendicular bone. Bone metastases are characterized as “lytic” (bone destructive), “blastic / sclerotic” (bone forming) or “mixed” according to the radiographic and/or pathologic appearance of the lesion. This classification represents the dysregulation of the normal bone remodeling process mediated by osteoblasts, osteoclasts and tumor cells.

Patients with breast cancer have predominantly osteolytic lesions (Trinkaus et al., 2009), although 15 to 20 percent of them have osteoblastic lesions. Bone metastases from kidney, lung or thyroid cancers more often are osteolytic. In addition, secondary formation of bone occurs in response to bone destruction. Only in multiple myeloma do purely lytic bone lesions develop. In contrast, the lesions in prostate cancer are predominantly osteoblastic. (Logothetis & Lin, 2005; Ye et al., 2007).

1.3 Clinical features

Bone metastases represent a major cause of morbidity and mortality, once tumors metastasize to bone they are usually incurable (Coleman et al., 2011). Bone metastases are rarely silent. They can give rise to a number of life-threatening complications (Coleman et al., 2006). Osteolytic metastases can cause severe pain, pathologic fractures, decreased mobility, hypercalcemia, anemia, spinal cord compression and other nerve-compression syndromes. Patients with osteoblastic metastases have bone pain and pathologic fractures because of the poor quality of the bone produced by the osteoblasts. Patients with fewer metastases or solitary lesions appear to have a better prognosis than those with multiple metastatic deposits.

1.4 Biomarkers of bone turnover

Biochemical markers of bone turnover have been used to assess the response to therapy or for the detection of bone metastases. Levels of bone-specific alkaline phosphatase, osteocalcin and type I procollagen C-propeptide are serum markers of osteoblast activity. Whereas, serum levels of C-terminal telopeptide of type I collagen or tartrate-resistant acid phosphatase and urinary levels of type I collagen cross-linked N-telopeptides are indicators of osteoclast activity (Roodman, 2004).

There are limitations to the clinical utility of many of these bone markers. Recently, some new markers have been described as potentially important role: CXXL16/CXCR6 (Ha et al., 2011), OPG/RANKL (Mercatali et al., 2011) or CCN3 (Ouellet et al., 2011).

2. Pre-clinical cancer research optical imaging modalities

Optical imaging is based on the detection of photons emitted from living cells, tissues or animals. It can be divided into bioluminescence imaging (BLI) and fluorescence imaging (FLI). The role of molecular imaging in pre-clinical research is evolving. In small animal models optical imaging technologies are used to visualize normal as well as aberrant cellular processes at a molecular-genetic or cellular level of function (Chaudhari et al., 2005; Kwon et al., 2010; Snoeks et al., 2011).

The mechanism for creating luminescent light is that luciferase, which acts as a catalyst in the presence of oxygen and ATP, converts chemical luciferin into oxyluciferin, releasing light in the process. The substrate D-luciferin is injected, distributes rapidly throughout the body of the animal and is taken up by the cells. The emitted light is detected by a cooled charged coupled device camera (CCD) and has a wavelength from 500 to 620 nm which is sufficient to penetrate small animal tissue (Ntziachristos et al., 2005).

As regards FLI, fluorescence occurs when the excited state is caused by external stimulation by light (Leblond et al., 2010). As for BLI, luminescence is caused by a chemical reaction (either a natural, biological one- bioluminescence, or a purely chemistry based one chemiluminescence) (Kim et al., 2010). Despite its distinctive features each modality revealed differences in sensitivity, signal-to-noise-ratio (SNR) and background emission from tissues. Autofluorescence of tissue reduces the signal-to-noise ratio, so in fluorescence imaging the SNR is expected to be greater than in bioluminescence imaging.

In vivo expression of reporter genes encoding bioluminescent or fluorescent proteins can be detected externally by sensitive detection systems. BLI could easily image in vivo a bone metastatic lesion that in the end-point histological analysis results in a tumor of $\approx 0.5 \text{ mm}^3$ volume, corresponding to $\approx 1.7 \times 10^4$ cells.

Optical imaging only provides semi-quantitative data because of tissue-dependent signal attenuation and poor positional information due to photon scattering. However, new advances have made it possible to extend BLI and FLI to 3D imaging by optical tomography, ensuring better quantification of photon emission. As a result of the development of fluorescence molecular tomography (FMT) and other 3D fluorescence and bioluminescence data capturing methods, it is now possible to acquire 3D optical data and use different modalities (radiography, μ CT, PET, SPECT or MRI) to ensure spatial resolution and anatomical detail (Nahrendorf et al., 2010).

The main advantage of optical imaging is by a noninvasive study its ability to visualize biological processes, such as angiogenesis, inflammation or matrix degradation in the development and growth of bone metastases (Snoeks et al., 2011).

3. Diagnosis imaging modalities: Algorithm choice

Imaging plays a major role given that early identification of skeletal metastases could lead to changes in patient management and quality of life. Imaging modalities are based on either direct anatomic visualization of the bone or tumor or indirect measurements of bone tumor metabolism (figure 1). Clinical evaluation demands multimodal diagnostic imaging owing to the limitations of the diagnostic techniques. Four main modalities are currently used in clinical practice: radiography, computed tomography (CT), scintigraphy and magnetic

resonance imaging (MRI). At present, positron emission tomography (PET) and single photon emission computed tomography (SPECT) have a potential for evaluation (Rybak et al., 2001; Costelloe et al., 2009).

These techniques differ in performance in terms of sensitivity and specificity, but none of the modalities alone seem to be able to yield a reliable diagnostic outcome. There is currently no consensus about the best modality for diagnosing the bone metastases and for assessing their response to treatment. In clinical practice, most oncologists do not even use the same criteria, which results in disparate assessments of bone metastases (González-Sistal, 2007; Welch & Black, 2010).

Although bone metastases can be treated, their response to treatment is considered “unmeasurable”, which excludes patients with cancer and bone metastatic disease from participating in clinical trials of new treatments (Hamaoka et al, 2010).

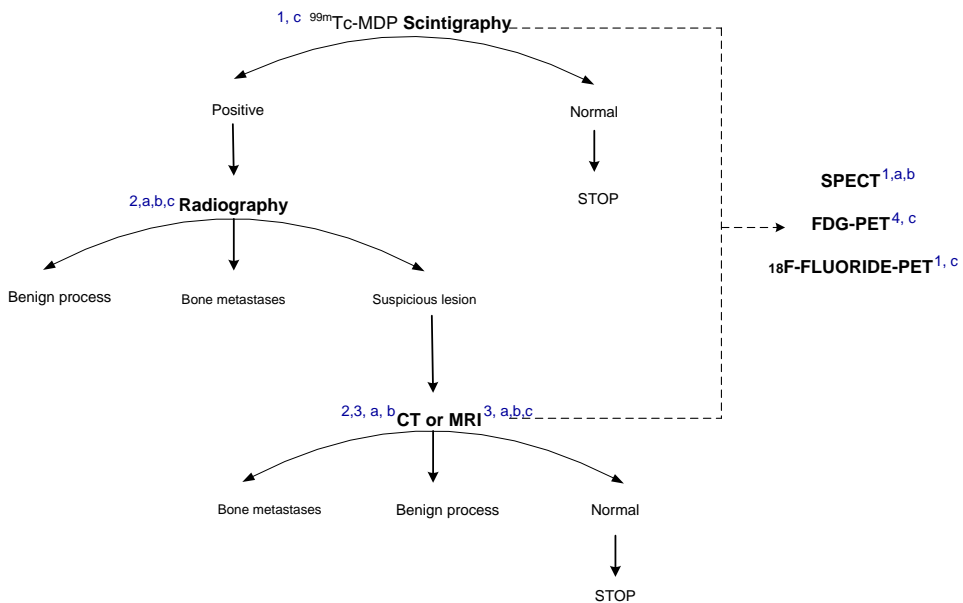


Fig. 1. Protocol for detection of bone metastases. Each imaging modalities visualize different aspects of bone tissue or tumor. (**Visualization:** 1 bone metabolism, 2 cortical/trabecular bone, 3 bone marrow / tumor, 4 tumor metabolism; **Extension:** a local, b regional, c whole body)

The algorithm of figure 1 shows a classical protocol for detection of bone metastases. The proposed algorithm is based in:

- Scintigraphy remains the technique of choice in asymptomatic patients in whom skeletal metastases are suspected (whole-body screening). This technique, albeit very sensitive, is poorly specific, and thus a bone scan finding is double-checked with an additional examination (radiography, CT or MRI).
- Radiography is used to evaluate symptomatic sites (bone pain) or confirm findings of other imaging modalities

- CT and MRI can depict anatomic changes in more detail. CT is preferable for assessing axial bone metastases, regardless of whether the main tumor involves the bone marrow or cortex. MRI, on the other hand, is better for detecting bone marrow disease or spinal cord compression.
- If MRI and CT cannot detect the disease and clinical suspicion of bone metastases remains, a PET/CT is made
- SPECT is not typically used for the initial detection of metastatic disease. SPECT-CT is useful for the assessment of lesions that are not determined in scintigraphy

4. Gamma-ray techniques

4.1 ^{99m}Tc -MDP bone scintigraphy

Bone scintigraphy is a nuclear medicine tomographic imaging technique using gamma rays. Technetium-99m bound to methylene diphosphonate (^{99m}Tc -MDP) is the most frequent radionuclide used in scintigraphy. The patient is injected this radiopharmaceutical and then he is scanned with a gamma camera (a device sensitive to the radiation emitted by the patient) which it produces a 2D picture.

^{99m}Tc -MDP bone scintigraphy is the method used to screen the whole body for bone metastases. It detects increases in osteoblastic activity and the flow of the blood level. It is a marker of bone turn-over or bone metabolism (Moore et al., 2007).

Scintigraphy is indicated for the following procedures: screening or staging in asymptomatic patients, evaluation of persistent bone pain with a negative radiography, determination of the extent of bone metastases in patients with positive radiography, differentiation of metastatic from traumatic fractures and determination of the therapeutic response to bone metastases (Hamaoka et al., 2004).

A classic pattern is the presence of randomly distributed focal lesions throughout the skeleton (figure 2) which appear as areas of increased tracer uptake ("hot spots"). Other typical patterns in scintigraphy are superscan (diffuse metastatic disease), cold lesions (due to complete absence of reactive bone, they are associated with aggressive carcinomas), normal scintiscan, flare phenomenon (osteoblastic activity that reflects bone healing after chemotherapy but not advancing disease) and hypercaptation in soft-tissue lesions.

As regards the degree of confidence, scintiscans are non specific for determining the cause of increased uptake (lower specificity) since the findings of scintigraphy reflect the metabolic reaction of bone. Bone scintiscans have a poor spatial and contrast resolution. Many benign processes can produce an isotope uptake that mimics metastases (false-positive finding) and approximately one third of patients show a solitary area associated with a benign process. Thus, biopsy confirmation may also be needed for the final diagnosis of suspicious lesions. The differential diagnosis includes metabolic illness, osteomalacia, trauma, arthritis, osteomyelitis, infarctions and Paget's disease. Therefore, suspicious lesions or a single "hot spot" should be verified by other imaging modalities such as radiography, CT, or MRI.

Scintigraphy does not detect pure lytic metastases when bone turnover is slow or when the site is avascular. The main advantages of scintigraphy are widely available and can screen rapid whole-body images at a reasonable cost.

When assessing the therapeutic response, scintigraphy should be supplemented by images obtained with other modalities to provide a valid baseline for the assessment of bone tumor. In addition, it can take six months or longer to detect a response in the scintigraphy because of the confounding effect of the flare phenomenon.

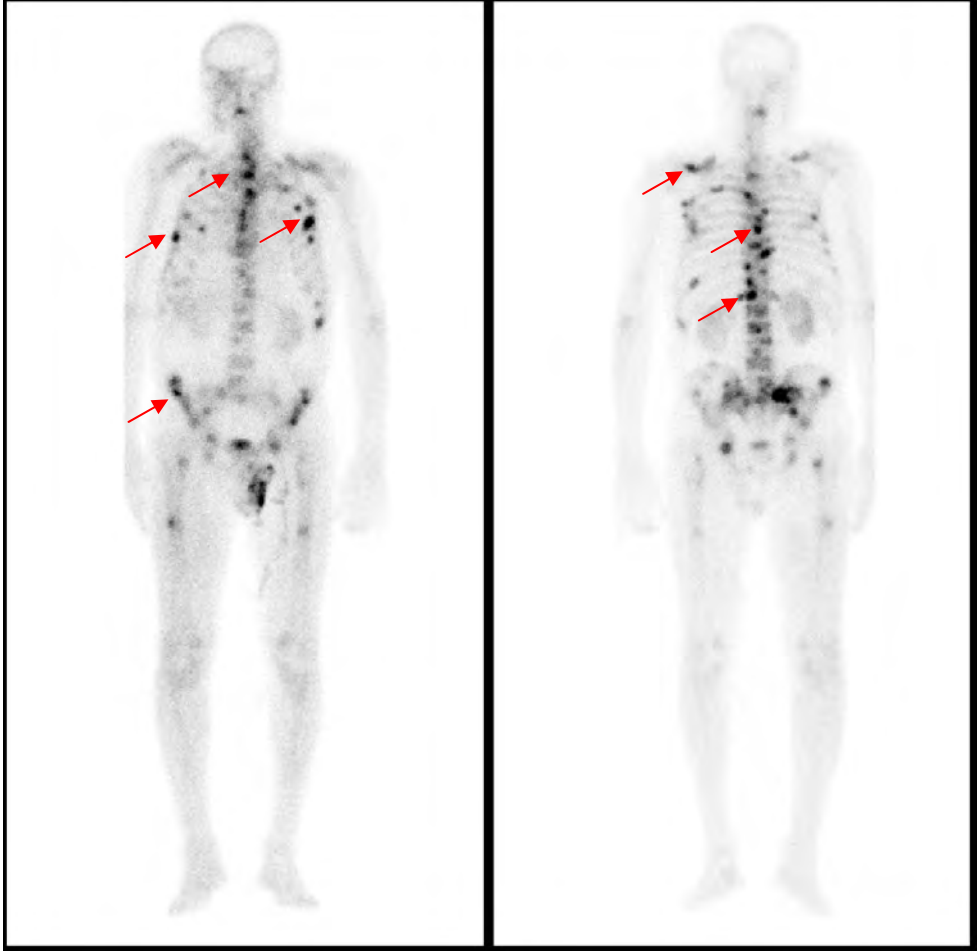


Fig. 2. ^{99m}Tc bone scintigraphy images of a patient with prostatic carcinoma. This is a classical pattern with the presence of randomly distributed focal lesions throughout the skeleton. Bone metastases appear as areas of increased tracer uptake (“hot spots”) (red arrows).

4.2 Single-photon-emission computed tomography (SPECT)

SPECT is a nuclear medicine tomographic imaging technique using gamma rays. ^{99m}Tc -MDP, the same radionuclide used in conventional skeletal scintigraphy is the most frequent radionuclide used. It is very similar to conventional nuclear medicine planar imaging using a gamma camera. However, images are acquired in a cross-sectional rather

than a planar fashion. It is able to provide 3D information. Compared with a conventional scintigraphy, the precise anatomic localisation provided by SPECT ensures a better differentiation between benign and malignant diseases. SPECT has greater sensitivity and specificity than scintigraphy for detecting vertebral and pelvis metastases (sensitivity 87-92% and specificity 73-100%). Like scintigraphy, it is possible that SPECT does not detect lytic lesions (Beheshti et al., 2009).

Because of limited availability and poor diagnostic imaging quality, SPECT is not typically used for the initial detection of metastatic disease (Chua, 2009). SPECT-CT is useful for the assessment of lesions that are not determined in scintigraphy. When scintigraphy are reviewed immediately, SPECT or SPECT-CT imaging can be performed in the same session without administering a second dose of radionuclide.

4.3 Positron emission tomography (PET)

PET is a nuclear medicine imaging technique that produces tomographic images through the detection of high-energy photon pairs emitted during positron decay of a radioisotope. PET visualizes the uptake of positron-emitting radioisotope by tissues, but, for skeletal metastases, two radiopharmaceuticals are typically used: ^{18}F -Fluoride, a bone turnover tracer, and ^{18}F FDG a tumor tracer. PET can be used for whole-body scanning to detect metastases in either soft tissue or bone. PET provides a 3D image of tracer concentration within the body that is then constructed by computer analysis. In modern scanners, 3D imaging is often accomplished with the CT or MRI on the patient in the same machine. PET has a limited spatial resolution and complementary CT scanning or MRI is required to localize the specific area (Costelloe et al., 2009; Cook, 2010).

Its main advantages are: high sensitivity (84-100%), biochemical and molecular information (does not always coincide with morphological explorations). PET is an effective technique that is used in the evaluation of skeletal metastatic disease, particularly when combined with CT, because of its high resolution and coverage of the whole body (Ben-Haim, 2009 & Israel, 2009). PET has the advantage of permitting quantification of therapeutic response using the maximum standard uptake (mSUV) value. PET can be a sensitive modality for diagnosing and monitoring osteolytic response (Beheshti et al., 2009; Wahl et al., 2009). However, the disadvantages may include PET cyclotron or the generator method, its high radiation, its high cost, its limited availability, and the additional time required for scanning with respect to other imaging modalities.

4.4 ^{18}F FDG-PET

^{18}F FDG (2-deoxy-2-[^{18}F]-fluoro-D-glucose or fluorodeoxyglucose) has been used to measure glucose metabolism in many types of primary cancer and can be useful for distinguishing benign from malignant bone lesions. It is an analog of glucose and represents the most widely used PET radiotracer in daily practice. The mechanism of uptake in tumor cells consist in the diffusion facilitated by glucose transporters (GLUTs), phosphorylation by hexokinase and subsequent metabolic trapping within the cell. It is a reflection of glucose metabolism consumption or tissue level.

Although it is a very sensitive marker, it is not very specific, since increases in tissue uptake of ^{18}F FDG is not always synonymous with cancer. The main clinical application of this

technique consists in diagnosing, staging and restaging of various cancer types (figure 3). It is very effective in detecting metastases of breast, lung, esophagus, colon, thyroid, head, neck, melanoma and lymphoma.

From the dosimetric point of view, it should be noted that an administration of 350 MBq of ^{18}F FDG results in a radiation exposure of approximately 6,3-7 mSv and PET/CT examination may result in a radiation exposure of more than 22-23 mSv, near the upper range of the dose given for regular diagnostic abdomen CT (3,5-25 mSv).

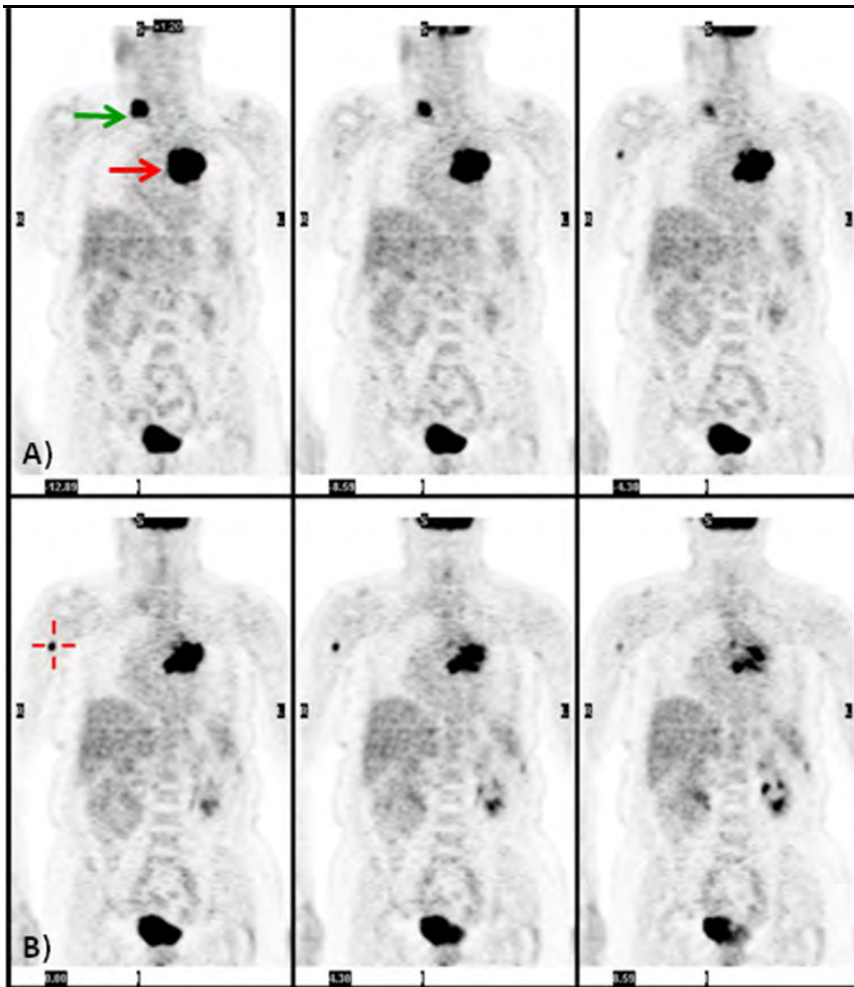


Fig. 3. PET images in a patient with lung carcinoma. **(A)** ^{18}F FDG PET shows the primary tumor (red arrow, 4x4.3cm, mSUV=27) with contralateral clavicle nodal metastases (green arrow, 2.7x2.5 cm, mSUV=19.2). **(B)** Incidental right humerus focal uptake is noted (red cross) which is suspicious for bone metastases modifying the initial disease staging from the patient to stage IV.

4.5 ^{18}F -fluoride-PET

The mechanism of ^{18}F -Fluoride uptake is similar to that of $^{99\text{m}}\text{Tc}$ -MDP, the tracer used in scintigraphy: its accumulation depends on osteoblastic activity and local blood flow. It is an indicator of bone turnover, but not of a specific tracer of bone metastases. At present, it is the second most commonly used technique in oncology, playing an important role in the detection of bone involvement. A number of studies have shown that the diagnostic accuracy of ^{18}F -fluoride-PET is better than scintigraphy (95,7% vs 75,4%) for detecting bone metastases in lung, prostate, thyroid and breast cancer, especially when using PET/CT (Withofs et al., 2011). Moreover, it appears to be more sensitive than SPECT.

The specificity of ^{18}F -Fluoride when used with PET alone is 62% (Groves et al., 2007), which demands a CT, mainly pelvic and lumbar injury, and may also detect extra-osseous metastases. An advantage is that it can detect early osteoblastic changes in slow growing tumors, where ^{18}F FDG has a limited value. ^{18}F -fluoride appears to be equally sensitive to osteoblastic and osteolytic metastases and can identify extremely early osteoblastic changes in response to metastatic deposits. It also seems to be superior in the detection the low avidity of bone tumor metastases for ^{18}F FDG as in some thyroid cancers.

Moreover, quantitative ^{18}F -Fluoride PET can determine kinetics of fluoride incorporation into bone as a measure of fluoride transport, bone formation and turnover. Kinetic analysis (fluoride transport and flux) may be useful in assessing changes in bone turnover in response to therapy, and in bone metastases with values exceeding those of normal bone (Doot et al., 2010).

5. X-ray techniques

5.1 Radiography

Radiography is an x-ray imaging technique that produces a 2D picture of human body structures superimposed on each other, whose insides absorb different amounts of radiation depending on the densities of its components. Bone metastases can appear on radiography as areas of absent density (osteolytic), as disrupted bone structure or as high density (osteoblastic). Radiography is a good method for characterizing bone metastases: osteolytic, osteoblastic or mixed. The occurrence of bone metastases suggests a primary tumor, eg. osteolytic metastases are typical in breast and lung carcinomas whereas osteoblastic metastases are more common in prostatic carcinoma (Hamaoka et al., 2004). Radiography is used to evaluate symptomatic sites (bone pain) or confirm findings of other imaging modalities (especially for evaluating suspicious lesions on scintigraphy). Radiography may be used to assess the risk of a pathological fracture. False positive diagnosis may result because osteolytic metastases can mimic osteoarthritis. Osteoblastic metastases may be difficult to distinguish from other sclerotic bone lesions such as tuberous sclerosis.

The disadvantage is that between 30 and 50% of normal bone mineral content must be lost before lytic lesions become apparent on radiography (Wahl et al., 2009). Moreover, lesions in trabecular bone are more difficult to detect by radiography than cortical. The main advantages of radiography are that it is cost effective and widely available. However, it is not recommended for screening because of its limited sensitivity, which depends partly on location (Rybal & Rosenthal, 2001).

Radiography can detect the response of osteolytic lesions by depicting active bone formation (blastic change) or the reappearance and normalization of bone structure. But, it may be difficult to differentiate bone metastases from healing or previously unidentified sclerotic lesions. In several studies, indicators of response to treatment on radiography are correlated with clinical symptoms or other changes better than scintigraphy. Nevertheless, changes in radiography are not apparent until three to six months after the initiation of treatment (Even-Sapir, 2005).

5.2 Computed tomography (CT)

CT consists of a large series of 2D x-ray images taken around a single axis of rotation. The computer assisted reconstruction is used to generate 3D pictures. The radiologic appearance in the CT bone window setting offers skeletal detail because it can distinguish between materials of different densities. It is more sensitive than radiography in the detection of bone metastases. CT is useful for evaluating radiography negative areas in symptomatic patients or where metastases are suggested clinically. CT is important in the evaluation of focal abnormalities observed in bone scintigraphy that cannot be confirmed using radiographs.

Osteolytic, osteoblastic and mixed bone metastases are well depicted on CT. It can detect metastases in the marrow. Bone metastases appear more attenuated than the marrow. But the usefulness of CT in detecting early deposits in bone marrow is limited. Although CT is superior to radiography some advanced destructive lesions on trabecular bone may not be visible in the absence of cortical bone involvement, so CT is less apparent than the marrow changes visualized on MRI (Hamaoka et al., 2004). CT is also better than radiography and scintigraphy for depicting lesions in the spine and calvarium. CT is useful in guiding needle biopsy in bones such as vertebrae or ilia.

The disadvantage of CT is that its high radiation dose makes CT unsuitable as a screening tool. Thus, limited anatomic areas can be scanned simultaneously (Rybal & Rosenthal, 2001).

When assessing the therapeutic response, sclerosis of a lytic component on CT suggests a response to treatment. Notwithstanding, lysis or the appearance of new lysis or an increase in the size of blastic lesion represents a disease progression (Hamaoka et al., 2009; Wahl et al., 2009).

5.3 Dual-energy X-ray absorptiometry (DXA)

DXA is a method for the evaluation of bone mineral density (BMD) and monitoring patients with osteopenia or osteoporosis, entailing minimal exposure to radiation (x-ray). Two x-ray beams with differing energy levels are aimed at the patient's bones. When soft tissue absorption is subtracted out, the BMD can be determined from the absorption of each beam by bone.

BMD reflects the balance between bone formation and resorption. This method has also been applied in several clinical trials to assess the therapeutic outcome of patients with bone metastases receiving systemic treatments (Vassiliou et al., 2011). The BMD of skeletal metastases increases in patients responding to treatment and was significantly correlated with the changes imaged on skeletal x-rays and CT.

6. Magnetic resonance imaging (MRI)

MRI produces high quality images of the inside of the human body. It uses a powerful magnetic field to align the magnetization of some atoms in the body (hydrogen nuclei or protons of the water molecules) and a radiofrequency fields to systematically alter the alignment of this magnetization. When a patient is subjected to the powerful magnetic field of the scanner, the magnetic moments of some of these protons change and align with the direction of the field. An image can be constructed because the protons in different tissues return to their state of equilibrium at different rates (tissue variables: spin density, T1 and T2 relaxation times, flow and spectral shifts) (Wu, 2011). Unlike the other techniques, MRI does not use ionizing radiation.

MRI diagnosis of bone metastases is characterized by long T1 relaxation times, whereas T2 relaxation times are variable, depending on tumor morphology. Metastases are seen as focal or diffuse areas of hypointensity on T1-weighted images which contrasts with the surrounding high signal marrow fat. Metastases can often be distinguished from focal deposits of red marrow because the latter are more focal and may have centrally located fat (bull's eye sign). In the case of T2-weighted images, bone metastases are seen as areas of intermediate or high signal intensity which contrast with normal marrow because of their high water content, and they are commonly, surrounded by a rim of bright signal (halo sign) (Schmidt, 2007).

MRI can identify bone metastases at an early stage. CT can also visualize bone marrow lesions, but the resolution is poor. The advantages of MRI include distinguishing benign (osteoporotic) from malignant causes of vertebral compression fracture, detecting spinal cord compression and the capability to obtain sagittal views of the entire spine to be assessed in one imaging session. Nevertheless, MRI is less advisable than radiography or CT for detecting the destruction of cortical bone structure because, cortical appears black on T1 and T2-weighted sequences.

Difussion-weighted imaging (DWI) is a MRI technique based on the imaging of molecular mobility of water (i.e. diffusion). Recently, DWI has been proposed as a time-and cost-effective detection to image tumor deposits throughout the whole body. DWI is considered a highly sensitive method for the detection of bone metastases (Luboldt, 2008; Takenaka, 2009).

With whole-body MRI, technical problems arise from the relatively long examination times (45–60 min) and the limited depiction of metastases in small bones. However, the development of ultrafast pulse sequences (Turbo STIR (short tau inversion recovery)) for whole-body MRI may substantially decrease imaging time. MRI scanning has contraindications, these include: pacemakers, metallic implants or ferromagnetic foreign bodies (e. g. shell fragments). Many benign process can produce the appearance of bone metastases on MRI (e.g in vertebral column: degenerative disk disease, osteomyelitis, benign compression fracture, infarcts or Schmorl's nodes).

When assessing the therapeutic response, MRI is optimal for showing spinal cord status and changes in the bone marrow but not suited to showing lytic or blastic change in bone structure.

7. Imaging modalities in major cancer entities

7.1 Breast cancer

The skeleton is the most common site of distant metastases in breast cancer (30%–85%). The vertebral column is the most common site of spread followed by the ribs. Bone metastases of breast cancer are lytic, blastic or mixed. Scintigraphy is indicated in patients with advanced disease or when bone involvement is clinically suspected. The use of ^{18}F -FDG PET it is not a routine staging procedure. ^{18}F -FDG PET allows for the detection of both soft-tissue and skeletal sites of disease. The superiority of ^{18}F -FDG PET was reflected mainly in the detection of bone metastases, which were predominately lytic. By using PET/CT, sclerotic lesions overlooked by the PET part of the study can be identified on the CT part. In this setting, the high sensitivity of ^{18}F -FDG PET for detecting marrow and lytic lesions and the high sensitivity of CT for detecting sclerotic lesions are complementary. Notwithstanding, some types of breast cancer, primarily well-differentiated histologic subtypes including some of the tubular and lobular ones, are less ^{18}F -FDG avid and so are their metastases. A recognized scintigraphy effect of antiestrogen therapy commonly applied in patients with breast cancer is the “flare reaction”. Clinically, it may be difficult to differentiate the flare reaction from disease progression. The initial agonist effect to therapy is also associated with increased tumor ^{18}F -FDG uptake. A change in ^{18}F -FDG uptake can be detected as early as 10 days after initiation of treatment compared with several weeks that are often required to make this assessment on the basis of clinical symptoms (Niikura et al., 2011).

7.2 Prostate cancer

Prostate cancer frequently metastasizes to bone (35-85%). Bone metastases of prostate cancer are predominantly blastic. The vertebral column (lumbar), pelvis, sternum, ribs and femur are the most common sites of spread. Staging of newly diagnosed prostate cancer is essential for guiding treatment. Patients with low-risk prostate cancer are unlikely to have metastatic disease on scintigraphy. Patients are referred for scintigraphy mainly if they are considered to be at high risk for bone metastases, with high PSA levels, a locally advanced disease, or a high Gleason score. Scintigraphy is the most widely used method for evaluating skeletal metastases of prostate carcinoma. The role of ^{18}F -FDG PET seemed to be limited in this type of cancer as both the soft-tissue sites of disease and bone metastases were reported to be ^{18}F -FDG negative or to show only a low-intensity uptake in many patients. PET/CT was suggested to overcome the problem of pelvic tumor sites being obscured by the radioactive urine. Using ^{18}F -FDG PET for monitoring the response to treatment, a decline in tumor glucose uptake measured as early as 48 h after androgen withdrawal, preceding any change in tumor volume or in PSA levels. Other PET tracers suggested for assessment of prostate cancer include ^{11}C - or ^{18}F -labeled choline and acetate, ^{11}C -methionine, ^{18}F -fluorodihydrotestosterone, and ^{18}F -fluoride. The latter may be highly sensitive for detecting bone metastases in patients with prostate cancer (Even-Sapir, 2007).

7.3 Lung cancer

Bone metastases are diagnosed at initial presentation in 4%–60% of patients with non-small-cell lung cancer (NSC). Bone pain is usually considered an indicator of skeletal metastases, but up to 40% of lung cancer patients with proven bone metastases are asymptomatic.

Surgical resection offers the highest probability of a favorable outcome in patients with NSC lung carcinoma. However, the survival of patients who undergo surgery remains low, probably because of presurgical understaging. Clinical staging at presentation has been performed by means of CT of the thorax through the liver and adrenals, CT or MRI of the brain, and scintigraphy for assessment of bone involvement. This staging algorithm remains the most commonly used in places where ^{18}F -FDG PET is not a routine staging modality of lung cancer. Including SPECT in the acquisition protocol of scintigraphy could improve the diagnostic accuracy scintigraphy in detecting bone metastases in patients with lung cancer. If necessary, scintigraphy can be complemented by CT or regional MRI for further assessment of unclear lesions. ^{18}F -FDG PET and PET/CT were recently reported to be of value in assessing the presence of soft-tissue and bone spread in patients with NSC lung cancer. They reported that ^{18}F -FDG PET had a high positive predictive value and a lower false-positive rate compared with scintigraphy (Even-Sapir, 2007).

The utility of PET in the detection of bone metastases is demonstrated in the following case (figures 4 and 5). A patient with lung carcinoma where the scintigraphy did not detect pure lytic metastases caused by slow bone turnover or an avascular site. The PET scan revealed a focus of increase FDG uptake suspicious for osteolytic metastases in the spine. MRI was requested for confirmation of diagnosis.

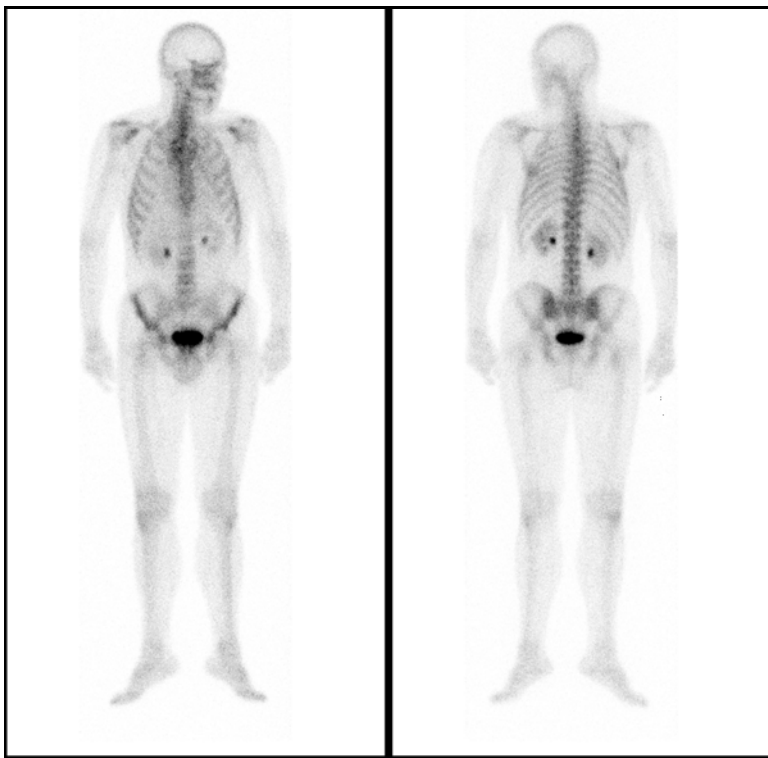
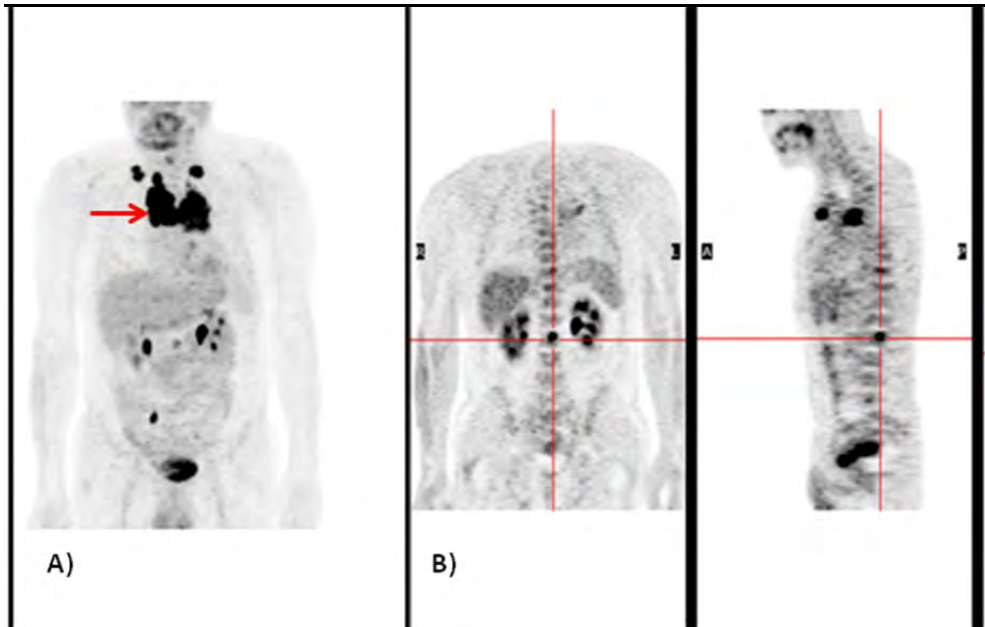


Fig. 4. $^{99\text{m}}\text{Tc}$ -MDP bone scintigraphy images of a patient with lung carcinoma. It is a normal scintiscan. The bone scan does not revealed suspicious foci of uptake



(A) PET show the primary tumor (red arrow). (B) A subsequent PET scan revealed a focus of increased FDG uptake in the spine (L2 vertebral body, red cross) which is suspicious for a osteolytic metastases.

Fig. 5. PET images in a patient with lung carcinoma. The utility of PET in the detection of bone metastases is demonstrated in this case. The bone scan, of the same patient, is showed in figure 4: a normal scintiscan (false negative case).

8. References

- Beheshti M, Langsteger W, Fogelman I. (2009). Prostate cancer: role of SPECT and PET in imaging bone metastases. *Semin Nucl Med* 39: 396-407
- Ben-Haim S, Israel O. (2009). Breast cancer: role of SPECT and PET in imaging bone metastases. *Semin Nucl Med* 39(6):408-15
- Chaudhari AJ, Darvas F, Bading JR, Moats RA, Conti PS, Smith DJ et al 2005. Hyperspectral and multispectral bioluminescence optical tomography for small animal imaging. *Phys Med Biol* 50:5421-5441
- Chua S, Gnanasegaran G, Cook GJR. (2009). Miscellaneous cancers (lung, thyroid, renal cancer, myeloma, and neuroendocrine tumors): Role of SPECT and PET in imaging bone metastases. *Semin Nucl Med* 39: 416-430
- Coleman RE. (2006). Clinical features of metastatic bone disease and risk of skeletal morbidity. *Clin Cancer Res* 15;12(20 Pt 2):6243s-6249s
- Coleman RE & McCloskey EV. (2011). Bisphosphonates in oncology. *Bone* 49(1):71-6
- Costelloe CM, Rohren EM, Madewell JE, Hamaoka T, Theriault RL, Yu TK, Lewis VO, Ma J, Stafford RJ, Tari AM, Hortobagyi GN, Ueno NT. (2009). Imaging bone metastases in breast cancer: techniques and recommendations for diagnosis. *Lancet Oncol* 10(6):606-14
- Cook GJ. (2010) PET and PET/CT imaging of skeletal metastases. *Cancer Imaging* 10: 1-8

- Doot RK, Muzi M, Peterson LM, Shubert EK, Gralow JR, Specht JM et al. (2010). Kinetic analysis of ¹⁸F-fluoride PET images of breast cancer bone metastases. *J Nucl Med* 51: 521-7
- Eriksen EF. (2010). Cellular mechanisms of bone remodeling. *Rev Endocr Metab Disord* 11(4):219-27
- Even-Sapir E. (2005). Imaging of malignant bone involvement by morphologic, scintigraphic, and hybrid modalities. *J Nucl Med* 46(8):1356-67
- Even-Sapir E. (2007). PET/CT in malignant bone disease. *Semin Musculoskelet Radiol* 11(4):312-321
- Fili S, Karalaki M, Schaller B. (2009). Mechanism of bone metastasis: the role of osteoprotegerin and of the host-tissue microenvironment-related survival factors. *Cancer Lett* 28;283(1):10-9.
- González-Sistal, A. Baltasar Sánchez, A (2006). A complementary method for the detection of osteoblastic metastases on digitized radiographs. *J Digit Imaging* 19(3):270-5
- González-Sistal A. (2007) Diagnostic Imaging Modalities of Osteoblastic Metastases *Hospital Imaging & Radiology Europe* 2 (1): 16-17
- Groves AM, Win T, Haim SB, Ell PJ. (2007). Non-[¹⁸F]FDG PET in clinical oncology. *Lancet Oncol* 8(9):822-30
- Ha HK, Lee W, Park HJ, Lee SD, Lee JZ, Chung MK. (2011). Clinical significance of CXCL16/CXCR6 expression in patients with prostate cancer. *Mol Med Report* 4(3):419-24
- Hadjidakis DJ, Androulakis II. (2006). Bone remodeling. *Ann N Y Acad Sci* 1092:385-96
- Hamaoka T, Madewell JE, Podoloff DA, Hortobagyi GN, Ueno NT. (2004) Bone imaging in metastatic breast cancer. *J Clin Oncol* 15;22(14):2942-53
- Hamaoka T, Costelloe CM, Madewell JE, Liu P, Berry DA, Islam R, Theriault RL, Hortobagyi GN, Ueno NT. (2010). Tumour response interpretation with new tumour response criteria vs the World Health Organisation criteria in patients with bone-only metastatic breast cancer. *Br J Cancer* 16;102(4):651-7
- Kim JB, Urban K, Cochran E, Lee S, Ang A, Rice B, Bata A, Campbell K, Coffee R, Gorodinsky A, Lu Z, Zhou H, Kishimoto TK, Lassota P. (2010). Non-invasive detection of a small number of bioluminescent cancer cells in vivo. *PLoS One* 23;5(2):e9364
- Kwon H, Enomoto T, Shimogawara M, Yasuda K, Nakajima Y, Ohmiya Y. (2010). Bioluminescence imaging of dual gene expression at the single-cell level. *Biotechniques* 48(6):460-2
- Leblond F, Davis SC, Valdés PA, Pogue BW. (2010). Pre-clinical whole-body fluorescence imaging: Review of instruments, methods and applications. *J Photochem Photobiol B* 21;98(1):77-94
- Logothetis CJ, Lin SH. (2005). Osteoblasts in prostate cancer metastasis to bone. *Nat Rev Cancer* 5(1):21-8
- Luboldt W, Kufer R, Blumstein N, Toussaint TL, Kluge A, Seemann MD, Luboldt HJ. (2008). Prostate carcinoma: diffusion weighted imaging as potential alternative to conventional MR and ¹¹C-choline PET/CT for detection of bone metastases. *Radiology* 249: 1017- 1025
- Mercatali L, Ibrahim T, Sacanna E, Flamini E, Scarpi E, Calistri D, Ricci M, Serra P, Ricci R, Zoli W, Kang Y, Amadori D. (2011). Bone metastases detection by circulating biomarkers: OPG and RANK-L. *Int J Oncol* 39(1):255-61
- Moore AE, Blake GM, Fogelman I. (2007). A study to determine the dependence of ^{99m}Tc-MDP protein binding on plasma clearance and serum albumin concentration. *Nucl Med Commun* 28(3):187-92

- Nahrendorf M, Keliher E, Marinelli B, Waterman P, Feruglio PF, Fexon L, Pivovarov M, Swirski FK, Pittet MJ, Vinegoni C, Weissleder R. (2010). Hybrid PET-optical imaging using targeted probes. *Proc Natl Acad Sci USA* 27;107(17):7910-5
- Niikura N, Costelloe CM, Madewell JE, Hayashi N, Yu TK, Liu J, et al (2011). FDG-PET/CT Compared with conventional imaging in the detection of distant metastases of primary breast cancer. *Oncologist*; 16 (8):1111-9
- Ntziachristos V, Ripoll J, Wang LV, Weissleder R. 2005 Looking and listening to light: the evolution of whole-body photonic imaging. *Nat Biotechnol* 23:313-320
- Ouellet V, Tiedemann K, Mourskaia A, Fong JE, Tran-Thanh D, Amir E, Clemons M, Perbal B, Komarova SV, Siegel PM. (2011). CCN3 impairs osteoblast and stimulates osteoclast differentiation to favor breast cancer metastasis to bone. *Am J Pathol* 178(5):2377-88
- Roodman GD. (2004). Mechanisms of bone metastasis. *N Engl J Med* 15;350 (16):1655-64.
- Rybak LD, Rosenthal DI. (2001). Radiological imaging for the diagnosis of bone metastases. *Q J Nucl Med* 45(1):53-64
- Schmidt GP, Schoenberg SO, Schmid R, Stahl R, Tiling R, Becker CR, Reiser MF, Baur-Melnyk A. (2007). Screening for bone metastases: whole-body MRI using a 32-channel system versus dual-modality PET-CT. *Eur Radiol* 17(4):939-49
- Snoeks TJ, Khmelinskii A, Lelieveldt BP, Kaijzel EL, Löwik CW (2011). Optical advances in skeletal imaging applied to bone metastases. *Bone* 48(1):106-14
- Suva LJ, Washam C, Nicholas RW, Griffin RJ. (2011). Bone metastasis: mechanisms and therapeutic opportunities. *Nat Rev Endocrinol* 7(4):208-18
- Takenaka D, Ohno Y, Matsumoto K, Aoyama N, Onishi Y, Koyama H, Nogami M, Yoshikawa T, Matsumoto S, Sugimura K. (2009). Detection of bone metastases in non-small cell lung cancer patients: comparison of whole-body diffusion-weighted imaging (DWI), whole-body MR imaging without and with DWI, whole-body FDG-PET/CT, and bone scintigraphy. *J Magn Reson Imaging* 30(2):298-308
- Trinkaus M, Ooi WS, Amir E, Popovic S, Kalina M, Kahn H, Singh G, Gainford MC, Clemons M. (2009). Examination of the mechanisms of osteolysis in patients with metastatic breast cancer. *Oncol Rep* 21(5):1153-9
- Vassiliou V, Andreopoulos D, Frangos S, Tselis N, Giannopoulou E, Lutz S. (2011). Bone Metastases: Assessment of Therapeutic Response through Radiological and Nuclear Medicine Imaging Modalities. *Clin Oncol (R Coll Radiol)* [Epub ahead of print]
- Wahl RL, Jacene H, Kasamon Y, Lodge MA. (2009). From RECIST to PERCIST: Evolving Considerations for PET response criteria in solid tumors. *J Nucl Med* 50 Suppl 1:122S-50S
- Welch HG, Black WC. (2010). Overdiagnosis in cancer. *J Natl Cancer Inst.* 5;102(9):605-13
- Weilbaecher KN, Guise TA, McCauley LK. (2011). Cancer to bone: a fatal attraction. *Nat Rev Cancer* 2011 Jun;11(6):411-25
- Withofs N, Grayet B, Tancredi T, Rorive A, Mella C, Giacomelli F, et al. (2011). 18F-fluoridePET/CT for assessing bone involvement in prostate and breast cancers. *Nucl Med Commun* 32: 168-76
- Wu LM, Gu HY, Zheng J, Xu X, Lin LH, Deng X, Zhang W, Xu JR. (2011). Diagnostic value of whole-body magnetic resonance imaging for bone metastases: a systematic review and meta-analysis. *J Magn Reson Imaging* 34(1):128-35
- Ye XC, Choueiri M, Tu SM, Lin SH. (2007). Biology and clinical management of prostate cancer bone metastasis. *Front Biosci* 1;12:3273-86